INTERFACE FOCUS

royalsocietypublishing.org/journal/rsfs

Research

Cite this article: Berthaume MA, Kupczik K. 2021 Molar biomechanical function in South African hominins *Australopithecus africanus* and *Paranthropus robustus*. *Interface Focus* 20200085.
https://doi.org/10.1098/rsfs.2020.0085

Accepted: 15 June 2021

One contribution of 14 to a theme issue 'Biological anthroengineering'.

Subject Areas:
bioengineering, biomechanics

Keywords:
dental biomechanics, *Paranthropus robustus*, *Australopithecus africanus*, three-dimensional printing, hominin evolution

Author for correspondence:
Michael A. Berthaume
e-mail: berthaume@lsbu.ac.uk

Electronic supplementary material is available online at rs.figshare.com.

THE ROYAL SOCIETY PUBLISHING

Molar biomechanical function in South African hominins *Australopithecus africanus* and *Paranthropus robustus*

Michael A. Berthaume[1,2] and Kornelius Kupczik[2,3]

[1]Division of Mechanical Engineering and Design, London South Bank University, 103 Borough Rd, SE1 0AA London, UK
[2]Max Planck Weizmann Center for Integrative Archaeology and Anthropology, and [3]Department of Human Evolution, Max Planck Institute of Evolutionary Anthropology, Leipzig, Germany

MAB, 0000-0003-1298-242X; KK, 0000-0003-1502-581X

Diet is a driving force in human evolution. Two species of Plio-Pleistocene hominins, *Paranthropus robustus* and *Australopithecus africanus*, have derived craniomandibular and dental morphologies which are often interpreted as *P. robustus* having a more biomechanically challenging diet. While dietary reconstructions based on dental microwear generally support this, they show extensive dietary overlap between species, and craniomandibular and dental biomechanical analyses can yield contradictory results. Using methods from anthropology and engineering (i.e. anthroengineering), we quantified the molar biomechanical performance of these hominins to investigate possible dietary differences between them. Thirty-one lower second molars were three-dimensional printed and used to fracture gelatine blocks, and Bayesian generalized linear models were used to investigate the relationship between species and tooth wear, size and shape, and biomechanical performance. Our results demonstrate *P. robustus* required more force and energy to fracture blocks but had a higher force transmission rate. Considering previous dietary reconstructions, we propose three evolutionary scenarios concerning the dietary ecologies of these hominins. These evolutionary scenarios cannot be reached by investigating morphological differences in isolation, but require combining several lines of evidence. This highlights the need for a holistic approach to reconstructing hominin dietary ecology.

1. Introduction

Diet is cited as the single most important factor underlying behavioural and ecological variation in extant primates [1]. As such, dietary reconstructions provide biological data about extinct primates. Short-term dietary reconstructions such as stable isotope and dental wear analyses provide data on behaviour and ecology on a (set of) population(s), while long-term dietary reconstructions such as morphological and biomechanical analyses provide data on the evolutionary history and functional adaptations of a species. Given their key role in mastication and relative abundance in the fossil record, a key element for reconstructing diet is postcanine dentition.

In Primates, the primary function of postcanine dentition is to decrease food item size. The mechanical transfer of force and energy from teeth to food plastically deforms and fractures the food, increasing its swallowability and digestibility [2,3]. If postcanine dentition cannot break down the food efficiently, primates are at risk of not obtaining enough calories for reproduction, lactation and/or survival [4]. The postcanine dentition has evolved in response to differences in extrinsic and intrinsic dietary properties to decrease food item size while resisting failure through excessive wear and fracture [2,5]. Quantification of tooth shape, size and biomechanical function allows researchers to estimate the biomechanical properties of the foods an animal is adapted to eat [2,6–10].

Two species of South African Plio-Pleistocene hominins—*Paranthropus robustus* and *Australopithecus africanus*—have derived craniomandibular and dental morphologies that are hypothesized to have evolved as biomechanical adaptations to distinct diets. The two most common short-term reconstructions for the Plio-Pleistocene mammals are stable carbon isotope and dental microwear (texture) analyses. Within herbivores, stable carbon isotope analyses inform on the photosynthetic pathways of the plants consumed. In Plio-Pleistocene continental Africa, this can be used to estimate the relative amount of savanna resource incorporated into an animal's diet. These studies, therefore, offer little information on the biomechanical properties of the foods consumed by *P. robustus* and *A. africanus* [11,12]. However, stable carbon isotope analyses suggest *A. africanus* may have consumed slightly more savanna dietary resources than *P. robustus* [13–17]. Dental microwear and dental microwear texture analyses provide insight into dietary biomechanics by quantifying differences in dental wear patterns, a product of dental kinematics and kinetics, which are hypothesized to be a product of bolus mechanical properties and dietary abrasives (e.g. phytoliths, dust, grit) [18–23]. Primates with 'tough' diets (i.e. diets requiring high levels of work) tend to have more scratches, while primates with 'hard' diets (i.e. diets requiring high forces) tend to have more pits, but the interpretation of microwear data is debated [24–26]. Thus, *P. robustus* is primarily reconstructed as consuming harder foods than *A. africanus*, but with significant dietary overlap [27–30].

Long-term hominin dietary reconstructions often focus on the form and biomechanical function of the masticatory apparatus. *Paranthropus robustus*'s relatively larger chewing muscles and orthognathic craniomandibular complex would have allowed it to produce a relatively higher bite force [31,32], while its more robust craniomandibular features, larger molars with strong, upright tooth roots and thicker enamel would have made it more efficient at resisting those forces [33–38]. Functional metrics of occlusal topography show *P. robustus*'s molars were relatively flatter [39], higher relief and morphologically better equipped to resist wear than *A. africanus's* [40]. Taken together, this suggests *P. robustus* was better adapted to resist the biomechanical loads brought on by mechanically challenging and/or harder foods [41]. Consistent with dental microwear studies, dietary reconstructions based on an adaptationist framework conclude *P. robustus* consumed more mechanically challenging and/or harder foods. There is debate about whether these foods were small and hard [42], low quality (requiring bulk feeding) [43] or underground storage organs (USOs) [44], and whether they were consumed regularly or seasonally [45,46]. Craniomandibular biomechanical analyses yield results consistent with the adaptationist interpretation [33,36,47,48].

Two occlusal dental biomechanics studies have investigated the dietary biomechanics of *P. robustus* and *A. africanus*, both of which focused on the ability of the two species to process hard foods [9,49]. These studies found *P. robustus* could fracture nuts with less force and energy than *A. africanus* [9], but *A. africanus* could resist the stresses induced by the point loads of small, hard objects more efficiently [49]. These studies suffered from small sample sizes, making it impossible to conclude if these differences were species or specimen specific, and modelling assumptions, as models of hard food item consumption are highly sensitive to initial food item placement.

Here, we use an anthroengineering approach to investigate the dental biomechanics of *P. robustus* and *A. africanus*. Anthroengineering is an interdisciplinary approach that uses theories and methods from anthropology and engineering to address questions within and across the respective disciplines. Here, we are combining mechanical engineering with palaeoanthropology to address a question concerning human evolution. We hypothesize *A. africanus*'s more sloped molars will increase its biting efficiency relative to *P. robustus*. If true, this would imply *A. africanus* could have consumed the same foods as *P. robustus*, but with less force or energy.

As a structure's geometry and biomechanical function are intrinsically linked, potential correlations between molar occlusal topography and biomechanical function are investigated. Experimental models of simple teeth (e.g. blade-like and unicuspid teeth, like incisors and canines) show there is a simple relationship between tooth shape and function that can be derived from first principles, as there is only a single or multiple symmetrical points of contact between the tooth and the food item [10,50–54]. However, experimental and finite element models have shown no simple relationship can be derived using first principles for complex teeth (e.g. multicusped bunodont molars that lack symmetry) due to multiple points of contact causing an asymmetric transfer of force/energy between the tooth and the food item [9,55]. Additionally, the percentage of total force transferred by each point of contact changes with food item size [56], adding an additional layer of complication to the problem.

Because of this, little is known about the complex relationship between molar shape and biomechanical function in primates. Presumably, functional metrics of occlusal topography (e.g. dental topographic metrics [8]) are linked to biomechanical performance, which is why primates with diets high in fibre or chitin have sharper teeth with relatively longer shearing crests—to improve cutting ability—while primates that consume hard foods have duller teeth—to improve crushing/grinding ability [6,57]. It is, therefore, possible some dental topographic metrics, like those used to quantify tooth sharpness or cutting ability (i.e. angularity [58] and Dirichlet normal energy (DNE) [8,59]) are correlated with metrics of biomechanical performance, like force or energy to fracture a food item. Currently, time consuming and potentially complex experiments/simulations are needed to elucidate the biomechanical function of complex teeth [9,60–62]. If a relationship between molar occlusal topography and biomechanical function can be established, it will allow for molar function to be estimated without the need for modelling.

2. Material and methods

2.1. Sample

As intact dental rows are rare in the hominin fossil record, we focus on a single tooth to expand our sample size and allow for statistical analysis. Lower second molars were chosen because (i) they are morphologically representative of the postcanine dentition [63,64], (ii) there is a strong relationship between M_2 shape and diet in Primates (e.g. [6,8,57,65,66]) and (iii) the relationship between tooth shape and diet is stronger in mandibular than maxillary teeth [67].

The sample in this study was from [40], with the exception that TM1600 was excluded due to large levels of dentin exposure. Briefly, 88 M_2s were considered and 31 relatively unworn M_2s were chosen for analysis (*A. africanus* = 17, *P. robustus* = 14; see

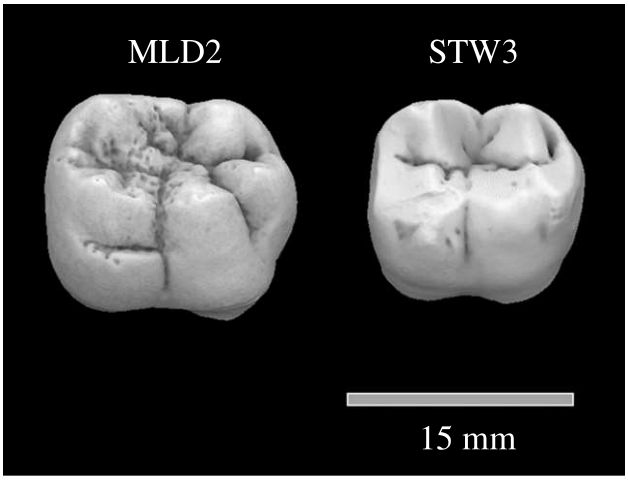

Figure 1. Lightly (MLD2) and moderately (STW3) worn *A. africanus* lower second molars considered for analysis. Although the fine features on the occlusal surface have been removed from STW3 due to wear, it still retains its general shape (e.g. cusp number and height).

electronic supplementary material, table S1). While we recognize our *A. africanus* sample here consists of some individuals classified as *A. prometheus* by Clarke and Kuman [68], we have not chosen to make the distinction between *A. africanus* and *A. prometheus* here. Relatively unworn molars with wear scores less than 6 [69] were chosen as dental wear changes tooth shape (figure 1) [40,58,70]. No antimeres were used.

2.2. Dental replicas

Digital surfaces of the teeth created for [40] were used to create dental replicas. Microcomputed tomography (microCT) scans were used to create digital representations of the teeth using a BIR Actis 300/255 FP or SkyScan 1172 microCT scanner at resolutions of 14–91 mm (see electronic supplementary material, table S1). MicroCT scans were processed in Avizo 8.1 (FEI, Hillsborough, USA) by thresholding, removing any matrix or bone touching the outer surface of the enamel cap, using the 'smooth labels' command (size = 3, 3D volume), and generating surfaces (smoothing type: existing weights). Surfaces files were imported into Geomagic Studio 2013 (3D Systems, Morrisville, USA), where the outer surface of the enamel cap was isolated and edited (e.g. smoothed, reconstructed and/or erasure of cracks; electronic supplementary material, table S1). When necessary and possible, portions of missing enamel were manually repaired in Geomagic Studio. Enamel caps were then imported into CloudCompare [71] and oriented into the anatomically correct position (i.e. how they would normally sit within the mandible), using fossils with portions of the mandible preserved as guides. Specimen specific deviations from the procedure detailed in this section can be found in the electronic supplementary material, table S1.

Enamel caps were reimported into Geomagic Studio and a rectangular column 2+ cm in height was drawn under each enamel cap. The rectangle's cross-sectional dimensions were altered such that, if the tooth was viewed from the occlusal surface, the rectangle could not be seen (figure 2). Portions of the rectangle closest to the enamel cap were deleted and attached to the enamel cap to create a water-tight volume using the 'Fill holes' function ('partial' and 'bridge' subfunctions). Accession IDs were engraved on the rectangle to allow for specimen identification after 3D printing. Teeth were then 3D printed in an Objet Eden 350 printer (Stratasys) using RGD720 at a resolution of 16 µm.

RGD720 is a nearly colourless, rigid transparent PolyJet photopolymer (Young's modulus = 2–3 GPa [72]). Although significantly more compliant than enamel/dentin, and therefore likely to deform under high forces, that was not a concern as the proxy food item used (gelatine) did not incur high reaction forces [73].

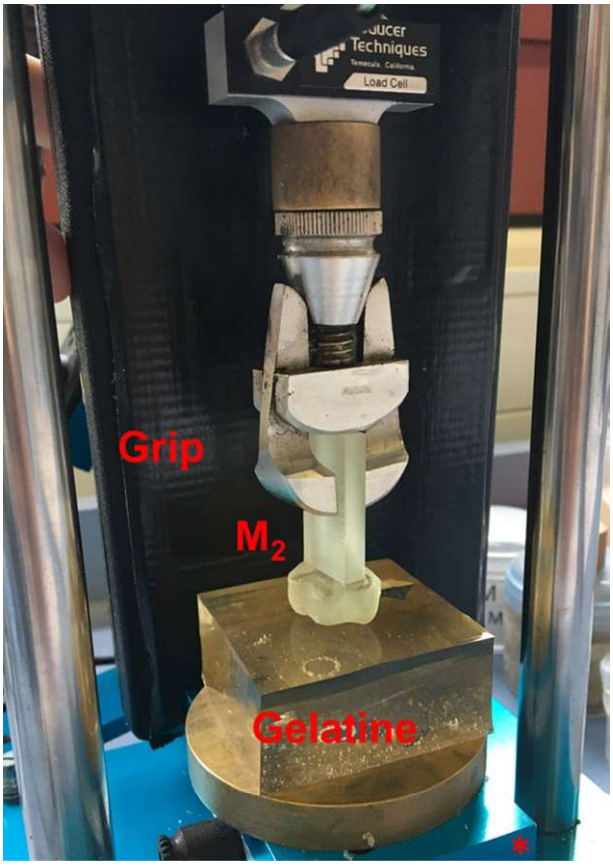

Figure 2. Experimental setup, showing a 3D printed tooth in the grips of the FLS II tester, above a gelatine block. Note: the blue rectangular base of the FLS II tester under the bronze round base (*) was used as the cutting guide for gelatine blocks.

2.3. Dental function

The dental biomechanical function was quantified using the dental replicas and proxy food items. Proxy food items were used to reduce the variation between trials [60,74]. Gelatine blocks were chosen as a proxy food item as their flat surfaces, hyperelastic behaviour and deformable nature meant they would mould to the occlusal surface of the tooth and be insensitive to initial food item placement. The results from these experiments better reflect whole-tooth biomechanical function. Preliminary trials were run to investigate the mechanical properties of gelatine, and ways to increase its energy release rate. Results from these trials are presented in electronic supplementary material, table S2. The final procedure used for all experiments is presented below.

Gelatine blocks were made by mixing 200.0 g (±0.1 g) of sucrose into 100 ml (±1 ml) of water in a sterilized beaker (70% ethanol). The solution was placed on a heated plate with a magnetic stirrer (200°C, 250 RPM) until the sucrose was dissolved. Meanwhile, a magnetic stirrer 75.0 g (±0.1 g) of gelatine was soaked in 400 ml (±1 ml) of water for 10 min. The swollen gelatine mixture was then heated and stirred (200°C, 250 RPM) until all the gelatine was dissolved. The sucrose solution was added to the gelatine solution and stirred for 2–3 min (200°C, 250 RPM). The mixture was then poured into two square, sterilized (70% ethanol) Pyrex glass containers with lids and placed in the fridge for at least 12 h. Prior to experimentation, gelatine blocks were cut into squares using the base of the FLS II tester as a guide and immediately used for experimentation (figure 2). Gelatine blocks were 47.5 mm wide and

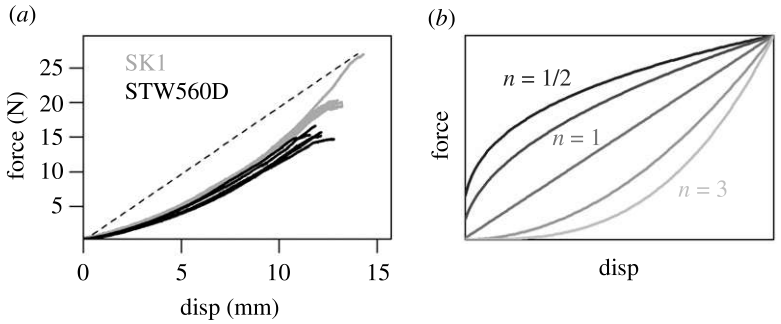

Figure 3. (*a*) Five biomechanical trials for SK1 (*Paranthropus robustus*) and STW560D (*Australopithecus africanus*). The dotted horizontal line is present to highlight the nonlinearity of the force–displacement curves. (*b*) Hypothetical force–displacement curves that fit the equation $F = x\text{^}n$, where the fracture occurs at a constant force and displacement in all curves. The area under the r-shaped curves is larger than the area under the J-shaped curves, indicating relatively more energy is needed to reach failure. From darkest to lightest curves, $n = 1/3$, 1/2, 1, 2 and 3.

21.05 ± 0.67 mm thick ($n = 74$ blocks) and had an energy release rate of 28.13 ± 7.06 J mm^{-2} ($n = 12$ trials, wedge test).

Dental replicas were placed in the grips of a motorized FLS II portable mechanical tester (Lucas Scientific) and lowered into the gelatine blocks until fracture at a constant displacement of 5.7 mm min^{-1} (figure 2). As in previous experiments, masticatory kinematics was simplified and modelled as a simple translation of the tooth in the occlusal direction [9,50,53,75,76]. Force and displacement were recorded at a data acquisition rate of 50 samples/second. Five trials were performed per dental replica. Experimental results were imported to Microsoft Excel 2016, where displacements were transformed such that a displacement of 0 mm corresponded to a force of 0.2 N. This is to compensate for the fact that the tooth and block were not in contact at the start of the experiment. All data past the maximum reaction force were removed. Both force and displacement at failure were recorded, and energy to failure was calculated using the right-hand rule from calculus.

The force–displacement curves produced during experimentation exhibited nonlinearity (figure 3); this is common in biological materials. This nonlinear relationship can be approximated with the following equation:

$$F = kx^n + F_0 \tag{2.1}$$

where F is the force, k is the effective stiffness, x is the displacement, n is a dimensionless coefficient quantifying curve shape and F_0 is the initial force (here, 0.2 N). When $n = 1$, the curve is linear. When $n > 1$, the force–displacement curve resembles an upper-case J and is thus referred to as 'J-shaped,' but when $n < 1$, the force–displacement curve resembles a lower-case r is thus referred to as 'r-shaped' [77,78] (figure 3). Assuming failure occurs at a given load and displacement, 'J-shaped' curves resist force more efficiently, displacement less efficiently and require less energy to fail than 'r-shaped.'

During these compression tests, changes in n occur because of changes in increase in density that occur as the material is compressed, where the material is applying a lower (in the case or r-shaped curves) or higher (in the case of J-shaped curves) reaction force per unit of displacement as the material is compressed. To solve for k and n requires the equation for work (W):

$$W = \int F\mathrm{d}x \tag{2.2}$$

Combining equations (2.1) and (2.2) and substituting 0.2 for F_0 gives

$$W = \int kx^n + 0.2\ \mathrm{d}x$$

$$W = \frac{kx^{n+1}}{n+1} + 0.2x + C$$

We can assume that $C = 0$ because, when $x = 0$, $W = 0$ as there is no work for zero displacement. Therefore

$$W = \frac{(F - 0.2)x}{n+1} + 0.2x$$

$$n = \frac{(F - 0.2)x}{W - 0.2x} - 1 \tag{2.3}$$

and

$$k = \frac{F - 0.2}{x^n} \tag{2.4}$$

where k has units of N m^{-n}. If the curve is linear ($n = 1$), k has units of N m^{-1}, the units commonly used to describe stiffness in elastic bodies. Maximum force, the corresponding displacement and energy to failure were used to calculate n and k using equations (2.3) and (2.4).[1]

Mastication is both force (i.e. bite force) and displacement (i.e. gape angle, tooth position and jaw length) limited. Given *P. robustus* has been proposed to have a more mechanically challenging diet than *A. africanus*, we hypothesize natural selection acted to produce a tooth morphology in *P. robustus* that could transmit forces more efficiently and fracture foods with relatively less force/energy than *A. africanus*: this is in concordance with the results from [9]. As such, we expect the force transmission rate to be higher in *P. robustus*, and the force/energy to fracture to be lower.

When force–displacement curves are linear, the force transmission is dictated solely by the effective stiffness of the system (k). In nonlinear curves, force transmission can be estimated by taking the derivative of force relative to displacement (i.e. the rate at which force is transmitted per unit displacement). The derivative of equation (2.1) is

$$\frac{\mathrm{d}F}{\mathrm{d}x} = nkx^{n-1} \tag{2.5}$$

where the force transmission rate has units of N m^{-1}. An interesting property of the force transmission rate is its dependence on n (figure 4). At very low displacements, force transmission rates are highest when $n < 1$ (r-shaped force–displacement curve) as the exponent for displacement, $n - 1$, is negative. As displacement increases, linear force–displacement curves ($n = 1$) provide the highest force transmission rate for a short time. When $n = 1$, force transmission rate is determined solely by k ($\mathrm{d}F/\mathrm{d}x = k$). As displacement increases, and for all displacements > 1 (mm in this case), force transmission rates are highest when $n > 1$ (J-shaped). This implies that, if a food requires a very small displacement to fail, teeth that produce r-shaped curves will be the most efficient at transmitting forces, but if a food requires a larger displacement to fail (here, any displacement greater than

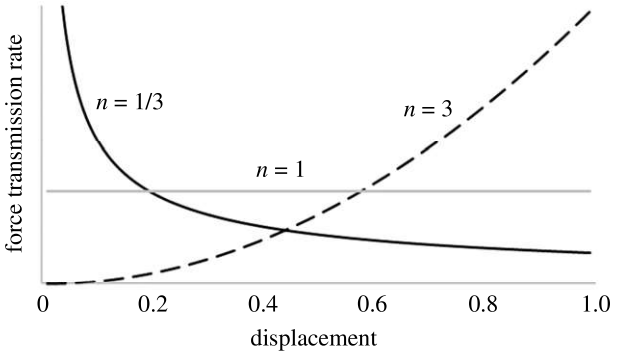

Figure 4. The effect of n on force transmission rate. At very low displacements, teeth that produce r-shaped force–displacement curves ($n < 1$) have the highest force transmission rate. At mid-level displacements, teeth that produce linear force–displacement curves ($n = 1$) have the highest force transmission rate. At high displacement, teeth that produce j-shaped force–displacement curves ($n > 1$) have the highest force transmission rate.

approx. 1 mm), teeth that produce J-shaped curves will be the most efficient at transmitting forces.

Here, we used displacement at fracture to calculate the force transmission rate.

2.4. Dental shape, size and wear

We used previously published data for tooth shape, size and wear, which is briefly described here [40]. Tooth shape was quantified with dental topographic metrics, which are correlated to ecological categories of diet in extant primates [8]. The metrics used here were (i) DNE, a measure of surface curviness which has been used to quantify tooth sharpness [6,59], (ii) relief index (RFI), a measure of relative tooth height [65,79], (iii) orientation patch count rotated (OPCR), a metric of dental complexity [80] and (iv) ambient occlusion (PCV, portion de ciel visible or 'portion of visible sky'), a metric of morphological wear resistance [81]. Five percentage outliers removal was used to calculate DNE (DNE 95% in [40]) to account for taphonomic artefacts in scans that may artificially inflate DNE. OPCR was calculated using 3D scans and is not directly comparable to values calculated using 2.5D scans, but the two measurements are correlated [40,81]. Tooth size was quantified using the projected outline area of the tooth [40,82]. Three metrics (DNE, RFI, OPCR) and tooth size were calculated in MorphoTester [82] and one (PCV) was calculated using CloudCompare [71]. Tooth wear was quantified using a modified method of Scott's dental scoring technique, where higher numbers indicate higher levels of wear [40,58,69,79].

When performing dental topography, surface files must be cropped to isolate the tooth for analysis. The cropping method must be held constant within a study, ensuring homologous portions of teeth are compared. The two most popular cropping methods were used here: the basin cut off (BCO) and the entire enamel cap (EEC) [8]. The BCO only considers portions of the tooth occlusal to an imaginary plane drawn through the lowest point on the occlusal basin. It thus only provides information about the occlusal surface of the tooth, and thus may be more related to food item breakdown than EEC, which considers the entire outer surface of the enamel cap. However, during experimentation, the sides of the tooth occasionally contacted the food item (figure 5), and thus EEC, which captures these aspects of morphology, may be more related to food item breakdown here. The cropping method not only affects the dental topographic results, but also tooth size, as the outline area is smaller when BCO is used, as the cervical margin of the tooth is not included. Tooth surfaces must be represented by approximately the same number of triangles, as several topographic metrics are sensitive to triangle count [83]. Here, triangle counts of 20 000 were used here [40,84].

2.5. Biomechanical statistical analyses

It is recommended first principles be used to derive testable hypotheses concerning the relationship between shape, size and performance in evolutionary biomechanics [85]. As discussed, this is not possible as there are no first principles relating complex tooth shapes (e.g. multicusped molars) or dental topography to biomechanical function [55,56,86,87]. Bayesian mixed-effects linear models were used to investigate whether differences in biomechanical performance existed between the two hominin species, and whether tooth shape, size or wear played a role in biomechanical performance. Mixed-effects models were used as they improve estimates for repeat sampling, improve estimates for imbalance in sampling, includes estimates of variation, and avoids averaging, retaining the experimental variation [88].

Using protocol set out by McElreath [88], we created six sets of equations, one for each biomechanical parameter (force, energy and force transmission rate), as well as displacement, k, and n as these are the parameters which drive the force transmission rate. The map2stan function was used in R to predict each biomechanical parameter using the following equation:

$$\begin{aligned}\text{Biomechanical parameter} = {} & \alpha + \alpha_{\text{trial}} + \alpha_{\text{specimen}} + \beta_1 * \text{DNE} \\ & + \beta_2 * \text{RFI} + \beta_3 * \text{OPCR} + \beta_4 * \text{PCV} \\ & + \beta_5 * \text{size} + \beta_6 * \text{wear} \\ & + \beta_7 * \text{species}\end{aligned}$$

Where broad, weakly regularizing priors were used to estimate α, α_{specimen} (the random effect individual fossils), α_{trial} (the random effect of trial number) and β_{1-7}. Markov-chain Monte Carlo (MCMC) estimation was used to estimate the posterior probability distributions for each parameter (4 chains, 10 000 iterations, 2000 iterations warmup). If one or more parameter appeared to be statistically insignificant, parameters were removed and additional models were run. Models were run using both BCO and EEC topographic results, and Watanabe–Akaike information criteria (WAIC) were used to compare all models and determine which set of parameters best predicted biomechanical performance: models with higher weights perform better. Random effects (trial, specimen), intercept (α) and species were included in all models. All statistical analyses were run in R v. 4.0.1 and RStudio using the rethinking package [88,89].

3. Results

As molars indented the gelatine blocks, the blocks conformed to the shape of the tooth (figure 5). When compressed to approximately 1/4 their thickness, cracks began to form in the blocks near the sides of the cusps, where the gelatine block was under tension (figure 5*d* and figure 6). While cracks occasionally form at the cusp tips, they often form next to the cusps, as the cusp tips are not sharp enough to propagate cracks through the gelatine blocks, and instead compress them. Eventually, crack(s) propagated through the gel, reducing the reaction force and causing failure. Specimen specific raw data are provided in figure 7 and electronic supplementary material, table S3. Results show a large level of overlap in biomechanical performance between *A. africanus* and *P. robustus*, but some species-level differences are present.

Apart from predicting k, WAIC weights showed the best Bayesian models for predicting biomechanical performance included species and tooth size, but not dental topographic parameters (table 1). Dental wear was important when predicting force, energy and k, but not displacement, n, or force transmission rate. WAIC weights indicate there was not always a clear best model for predicting biomechanical

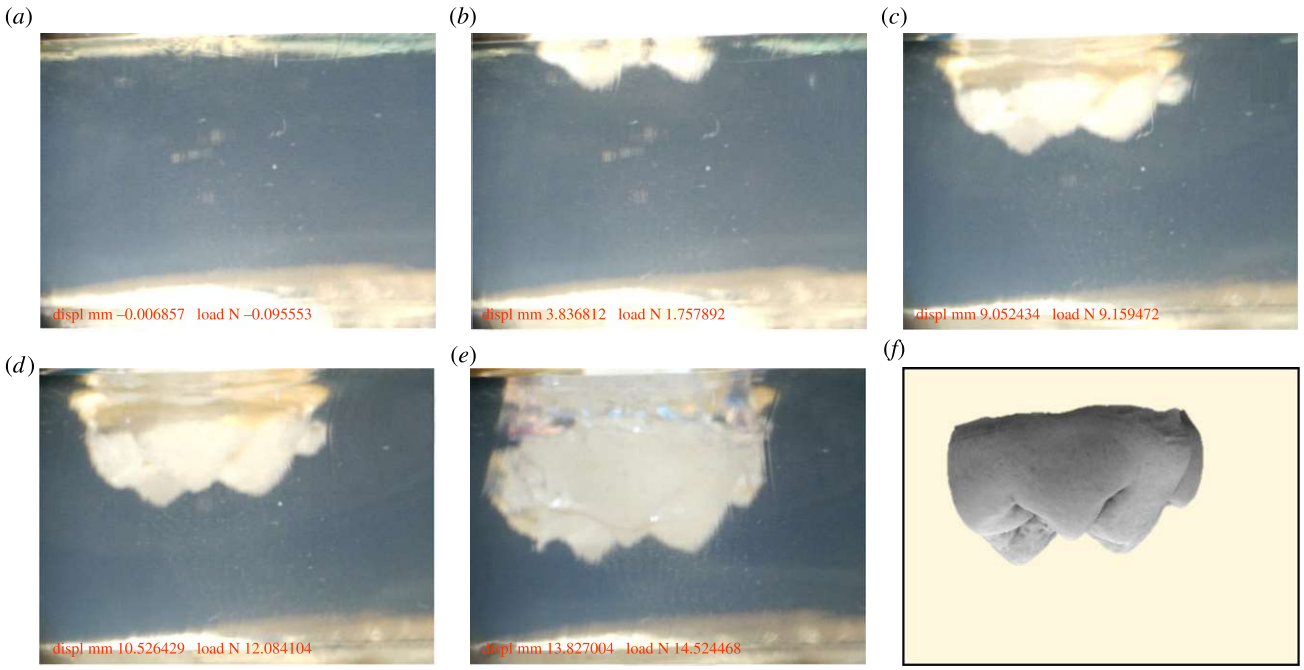

Figure 5. (*a–e*) Example of a 3D printed tooth (LM2, MLD2) indenting into and fracturing the gelatine blocks. Small fractures occurred in the gelatine blocks prior to catastrophic failure (e.g. *d*) and at catastrophic failure (*e*), as indicated by the reflective surfaces within the gelatine block, radiating from the tooth. Orientation of the tooth at time of fracture (*f*).

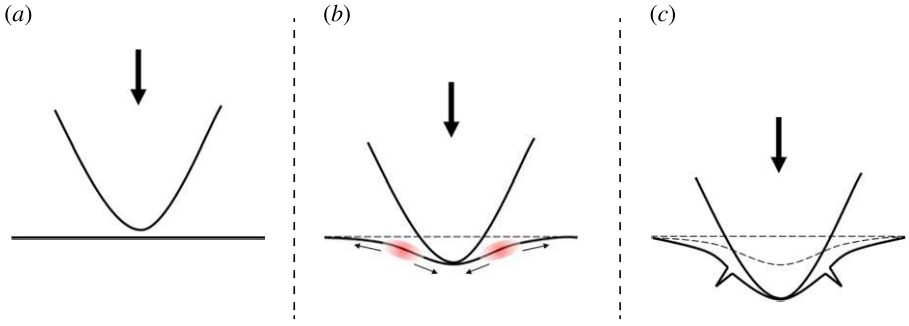

Figure 6. (*a–c*) Hypothetical cusp fracturing a gelatine block. As the gelatine is compressed, areas of high tension occur on the surface of the gelatine (as indicated by arrows and red areas in *b*). Ultimately, one or more of these areas fracture (*c*). Fractures can be small (e.g. figure 5*d*) or large, causing catastrophic failure.

performance. The best statistical models for predicting displacement, *k*, *n* and force transmission rate used data gathered using the BCO cropping method, while the best model for predicting force and energy used data gathered using the EEC cropping method, implying there is no single metric of tooth size that is best for predicting biomechanical performance. Summary statistics for the posterior distributions are available in table 2, electronic supplementary material, figure S1 and table S4. The code for the models is presented in electronic supplementary material, table S5.

Paranthropus robustus required more force and energy than *A. africanus* to fracture the gelatine blocks and had a higher force transmission rate (table 3). There were no differences in displacement, *k* or *n*. For both species, tooth size was positively correlated to displacement, force and energy to fracture the gelatine blocks: every 1 mm^2 increase in tooth size corresponded to 0.018 mm increase in displacement, 0.134 N increase in force and 0.673 mJ increase in energy to fracture. Larger teeth increased force transmission rate and n, making the force–displacement curves more J-shaped, but decreased *k*. Tooth wear increased the force and energy to fracture the gelatine blocks. Dental topographic metrics were never statistically significantly correlated to biomechanical performance.

Species averages for all biomechanical metrics were estimated using the best statistical models. As species averages change with tooth size and/or wear, estimates for various tooth sizes and/or wear stages are provided in the electronic supplementary material. Excluding the exceptionally large Gondolin molar, the range of tooth sizes using the EEC cropping method was 157.538–236.895 mm^2 and 159.765–239.38 mm^2 for *A. africanus* and *P. robustus*, respectively. Using the BCO cropping method, the range of tooth sizes were 143.084–198.405 mm^2 and 138.175–225.071 mm^2 for *A. africanus* and for *P. robustus*, respectively. As such, the biomechanical results presented here are for a tooth size of 195 mm^2 for force and energy and 175 mm^2 for displacement, *k*, *n* and force transmission rate. A wear stage of 1 was used when needed.

Paranthropus robustus required an average of 31.7% more force and 20.9% more energy to fracture the gelatine blocks than *A. africanus*. *P. robustus*'s force transmission rate was an average of 24.2% higher (table 3).

4. Discussion

Paranthropus robustus were relatively less efficient at fracturing the gelatine blocks than *A. africanus*, requiring more

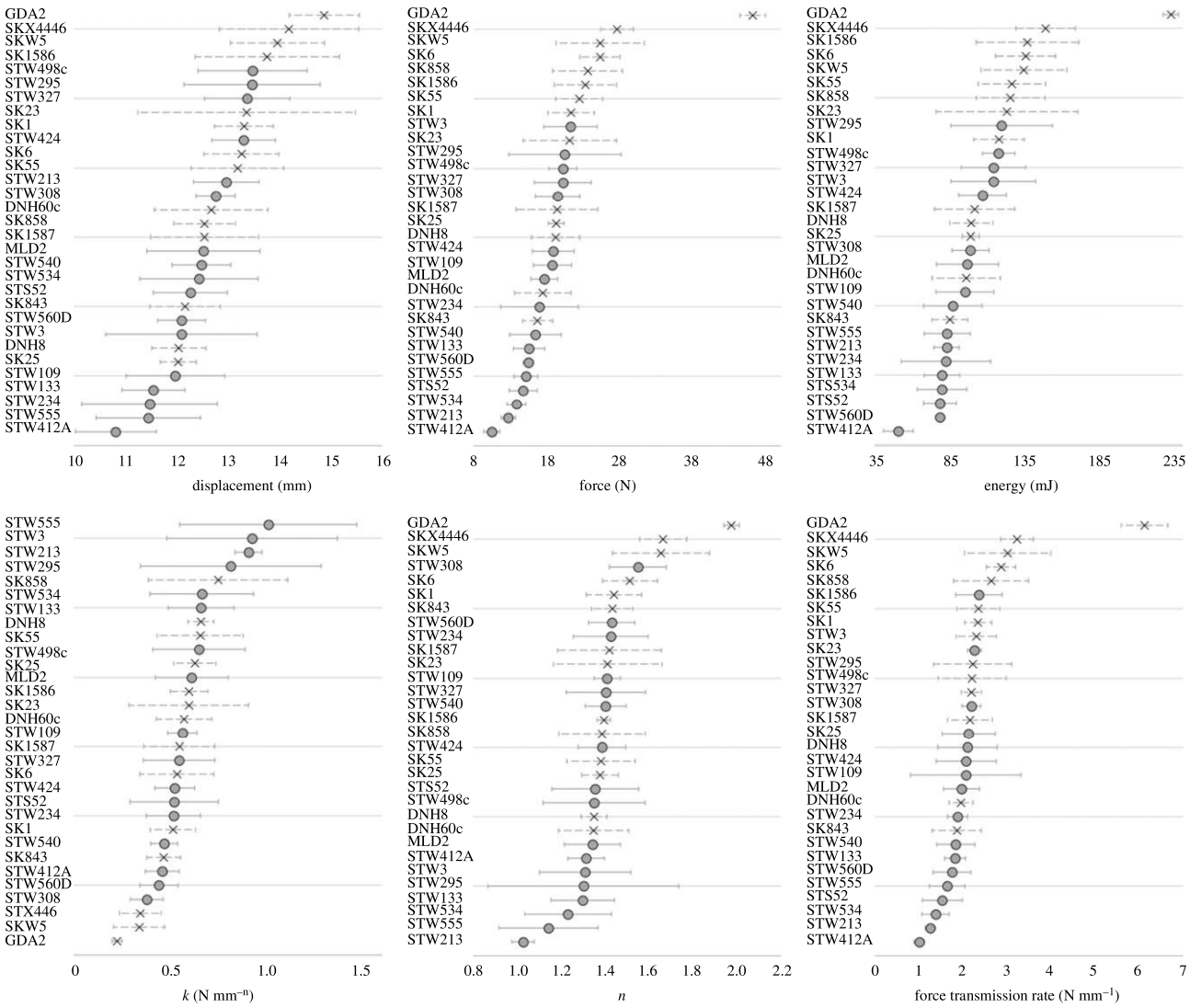

Figure 7. Specimen means and standard deviations across the five trials. Fossil accession IDs are listed on the left. Grey circles are *Australopithecus africanus*, and black X's are *Paranthropus robustus*. Error bars represent one standard deviation.

force and energy, but possessing a higher force transmission rate, allowing there to be no differences in failure displacement. Results indicate that, if *P. robustus* and *A. africanus* consumed the same foods, *P. robustus* would have required a similar gape but more force and energy, although there is significant overlap in the results of the two taxa. This could be accomplished by *P. robustus* having larger muscles and/or higher mechanical advantage, which would require *P. robustus* to have relatively thicker enamel to resist those forces/energies [31–38].

Under this scenario, the differences in craniomandibular morphology, relative tooth size and molar enamel thickness between these two hominins may not indicate adaptations to different diets, but rather adaptations to compensate for differences in dental biomechanical performance. This conclusion cannot be reached by investigating morphological differences in isolation and can only be seen by taking a more holistic approach.

What is causing this difference in dental biomechanical performance cannot be said for certain, but they are not related to DNE, RFI, OPCR or PCV. Unfortunately, these topographic parameters are uncorrelated to biomechanical performance (e.g. figure 8). This is expected when the EEC cropping method is used, as portions of the tooth that are not contacting the food item are being quantified. Yet, this is unexpected when the BCO cropping method is used, as only the occlusal surface is being quantified. This runs contrary to our understanding of these metrics [6,59,66,70,90]. Both DNE, a measure of surface curvature and metric of dental sharpness, and OPCR, a measure of the number of 'tools' on a tooth's surface, are hypothesized to correlate with masticatory efficiency [6,8,59,80,91–93]. Current hypotheses concerning dental function speculate DNE and OPCR are negatively correlated to force/energy to fracture foods: we found no such correlation here. It is possible DNE and/or OPCR are related to aspect(s) of biomechanical performance not captured by these experiments, such as chewing efficiency (i.e. the ability to fracture food into smaller pieces). Previous experimental results have shown chewing efficiency is correlated with relative shearing crest length in three species of small mammals [64,94,95], making it possible it is also correlated to other aspects of tooth shape. However, no research has shown a relationship between DNE or OPCR and chewing efficiency. Results from this paper highlight our lack of understanding of occlusal dental biomechanics in multicusped complex teeth [8].

If natural selection is the primary evolutionary force responsible for hominin molar morphology, dental biomechanical

Table 1. Results for the WAIC showing the effects of including the random effects of species on predicting energy from tooth size. WAIC is the WAIC score for each model, pWAIC is the effective sample size, dWAIC is the difference in WAIC values, weight is the Akaike weight (the estimate of the probability that the model will make the best predictions on the new data), SE is the standard error of the WAIC estimate and dSE is the standard error of the difference in WAIC.

	cropping method	species	wear	size	DNE	RFI	OPCR	PCV	WAIC	SE	dWAIC	dSE	pWAIC	weight
displacement	BCO	X	0	X	0	0	0	0	438.1	22.47	0	na	24.8	0.45
	EEC	X	X	X	0	0	0	0	438.9	22.36	0.8	1.23	25.4	0.3
	EEC	X	X	X	X	X	X	X	440.4	22.8	2.4	2.76	26.6	0.14
	BCO	X	X	X	X	X	X	X	440.9	22.73	2.8	2.23	27	0.11
force	EEC	X	X	X	0	0	0	0	823.9	22.79	0	na	28.8	0.31
	BCO	X	0	X	0	0	0	0	824.1	22.89	0.2	1.9	28.9	0.27
	BCO	X	X	X	X	X	X	X	824.4	22.78	0.6	1.43	29.1	0.23
	EEC	X	X	X	X	X	X	X	824.8	22.44	0.9	1.9	29.4	0.19
energy	EEC	X	X	X	0	0	0	0	1386.2	23.92	0	na	27.5	0.33
	BCO	X	0	X	0	0	0	0	1386.9	23.86	0.7	2.98	27.9	0.23
	EEC	X	X	X	X	X	X	X	1386.9	23.75	0.7	2.47	27.7	0.23
	BCO	X	X	X	X	X	X	X	1387.1	24.04	0.9	1.61	27.8	0.21
k	BCO	X	X	X	X	X	X	X	−17.2	27.5	0	na	25	0.33
	BCO	X	0	X	0	0	0	0	−16.9	28.09	0.3	4.87	25.4	0.28
	EEC	X	0	X	0	0	0	0	−16.4	28.17	0.9	4.77	26	0.21
	EEC	X	X	X	X	X	X	X	−16	27.32	1.2	3.43	26	0.18
n	BCO	X	0	X	0	0	0	0	−106.2	23.02	0	na	24.4	0.41
	BCO	X	X	X	X	X	X	X	−105.9	23.37	0.3	1.77	24.6	0.36
	EEC	X	X	X	X	X	X	X	−104	23.67	2.2	3.05	26.1	0.13
	EEC	X	X	0	0	0	0	0	−103.1	23.53	3.1	2.63	26.9	0.09
force transmission rate	BCO	X	0	X	0	0	0	0	254.7	23.08	0	na	29	0.33
	EEC	X	0	X	0	0	0	0	254.8	23.21	0.1	1.39	29.1	0.31
	BCO	X	X	X	X	X	X	X	255.7	22.85	1	2.27	29.7	0.2
	EEC	X	X	X	X	X	X	X	256	22.53	1.3	2.19	29.9	0.17

rsfs20200085—24/6/21—16:59—Copy Edited by: Not Mentioned

Table 2. Summary statistics for the posterior distributions for the fixed effects of the best models, according to WAIC results. *p*-values indicate the significance of the parameters, and values less than 0.05 are highlighted in italics. There were no differences between *P. robustus* and *A. africanus* in displacement, *k* or *n*. *P. robustus* was coded as '1' and *A. africanus* as '0' so a positive value indicates *P. robustus* had higher values for that biomechanical metric.

biomech. metric	parameter	mean ± s.d. (95% CI)	two-tail *p*-value (*p*-values of 0 are $< 3.125 \times 10^{-5}$)	effective sample size
disp.	species	0.453 ± 0.273 (−0.079 to 0.991)	0.094	11551.81
	tooth size	0.018 ± 0.005 (0.008 to 0.028)	*0.002*	9869.579
	intercept	9.341 ± 0.953 (7.447 to 11.214)	*0*	9301.876
force	species	4.76 ± 1.285 (2.201 to 7.296)	*0.001*	8282.971
	wear	1.223 ± 0.491 (0.252 to 2.201)	*0.017*	8324.856
	tooth size	0.134 ± 0.022 (0.091 to 0.178)	*0*	8084.333
	intercept	−12.335 ± 4.781 (−21.795 to −2.961)	*0.012*	7249.449
energy	species	17.198 ± 5.753 (5.533 to 28.089)	*0.006*	10860.04
	wear	7.856 ± 2.572 (2.818 to 13.022)	*0.003*	9435.137
	tooth size	0.673 ± 0.11 (0.454 to 0.889)	*0*	9693.009
	intercept	−55.569 ± 23.902 (−102.599 to −8.115)	*0.023*	8973.629
k	species	0.014 ± 0.076 (−0.135 to 0.165)	0.857	13669.67
	wear	−0.008 ± 0.049 (−0.105 to 0.09)	0.874	12782.29
	tooth size	−0.003 ± 0.001 (−0.006 to −0.001)	*0.007*	18579.66
	DNE	−0.001 ± 0.001 (−0.002 to 0.001)	0.514	15560.68
	RFI	1.726 ± 1.703 (−1.672 to 5.126)	0.301	11057.16
	OPCR	0.002 ± 0.001 (0 to 0.004)	0.1	17857.1
	PCV	2.07 ± 2.362 (−2.637 to 6.726)	0.368	9545.839
	intercept	−0.815 ± 1.853 (−4.484 to 2.848)	0.649	9647.519
n	species	0.086 ± 0.046 (−0.003 to 0.177)	0.058	13351.73
	tooth size	0.004 ± 0.001 (0.002 to 0.005)	*0*	13779.07
	intercept	0.699 ± 0.162 (0.379 to 1.018)	0.989	10843.26
force trans. rate	species	0.692 ± 0.208 (0.285 to 1.101)	*0.032*	6478.685
	tooth size	0.018 ± 0.004 (0.011 to 0.025)	*0*	5471.471
	intercept	−1.744 ± 0.758 (−3.261 to −0.249)	*0.009*	5144.656

Table 3. Species averages for biomechanical metrics.

	p-value	*P. robustus* median (95% CI)	*A. africanus* median (95% CI)
disp (mm)	0.094	12.914 (12.249–13.535)	12.460 (11.803–13.053)
force (N)	0.001	19.823 (16.521–23.029)	15.056 (12.218–17.921)
energy (mJ)	0.006	100.888 (84.865–116.251)	83.445 (68.807–98.275)
k (N mm^{-n})	0.857	0.559 (0.430–0.693)	0.617 (0.496–0.748)
n	0.058	1.435 (1.304–1.554)	1.350 (1.222–1.463)
force transmission rate (N mm^{-1})	0.032	2.393 (1.914–2.871)	1.927 (1.490–2.371)

analyses reveal how natural selection acted on hominin molar morphology in the past. Biomechanical analyses further reveal the limitations of dental function, and therefore the evolutionary constraints hominin molars would have been functioning within.

Given data from this study, as well as dental microwear, stable carbon isotope, and morphological dietary reconstructions, we propose three possible evolutionary scenarios concerning the biomechanical properties of the foods consumed by *P. robustus* relative to *A. africanus*:

(1) *P. robustus*'s diet was more mechanically challenging than *A. africanus*, and the selective pressure(s) related to bite force/energy were relaxed in *P. robustus*.

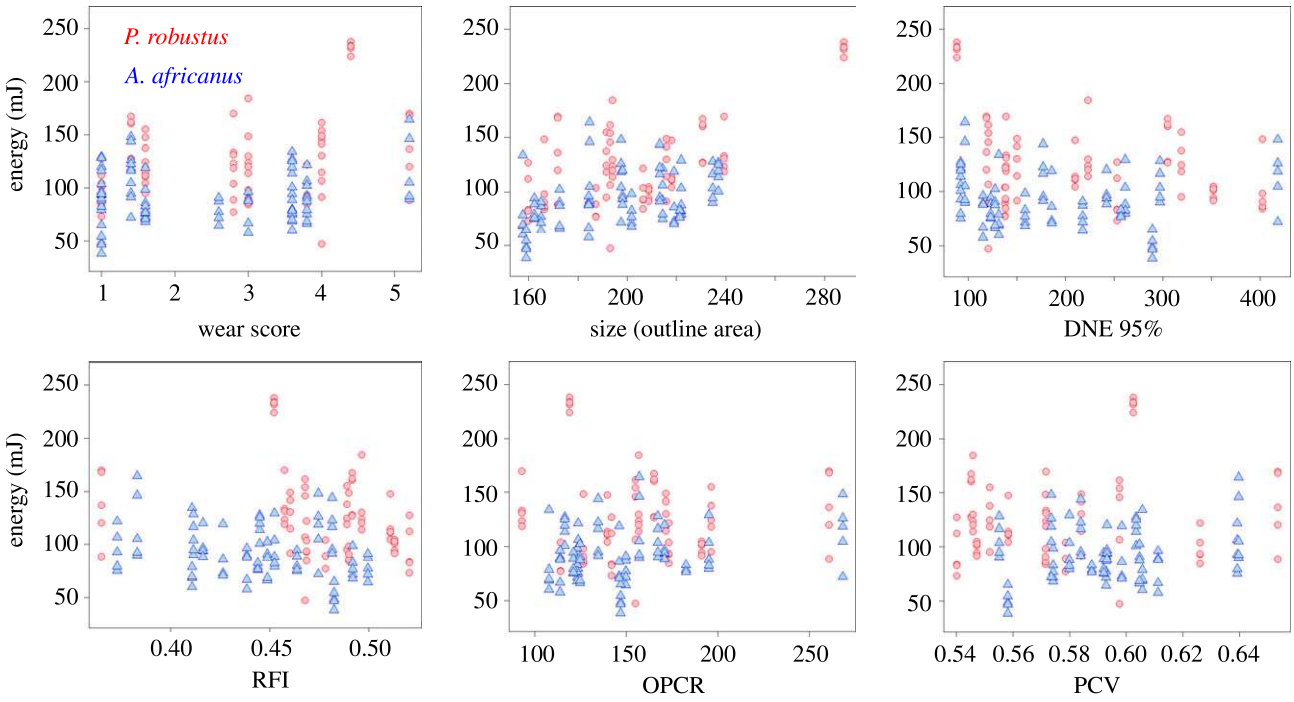

Figure 8. Raw data from experiments, showing energy versus tooth wear, size and four dental topographic parameters (EEC, triangle count = 20 000). Red circles are *P. robustus*, blue triangles are *A. africanus*.

If *P. robustus*'s diet was more mechanically challenging [27,28,33,96], results from this study suggest selection was not acting on occlusal topography to increase biomechanical performance during biting. This could be because having lower bite force/energy did not increase reproductive fitness within *P. robustus*, and therefore the selective pressures acting on dental biomechanics were relaxed. Musculoskeletal energetics and thereby force production are important when energy expenditure represents a large portion of an animal's energy budget (e.g. locomotion). Relative to these larger energy expenditures, it is possible the energy required to grow and maintain larger chewing muscles and/or to process foods was relatively unimportant in *P. robustus* [97]. Given an infinite population and infinite amount of time, natural selection will optimize all aspects of morphology, regardless of the strength of the selective pressure. If hypothesis 1 is true, it is possible that, in the case of the South African hominins, the population size was not large enough and/or not enough time has passed for bite force/energy during mastication to be optimized.

(2) *P. robustus*'s diet was more mechanically challenging, but selective pressures acted on the aspect(s) of dental morphology unrelated to bite force/energy in *P. robustus*.

As a result of natural selection acting on aspects of dental morphology unrelated to masticatory function, *P. robustus* evolved molars that were relatively inefficient at processing foods. One aspect of dental morphology selection could have been working on is molar enamel thickness. Molar enamel thickness is an adaptation to both dietary and environmental factors, and is highly correlated to primate growth and development [5,98–101]. Within primates, enamel thickness has been shown to be correlated with occlusal topography [102,103], so it is possible changes in enamel thickness in response to environmental and/or growth and development factors led *P. robustus* to have biomechanically inefficient molars.

(3) *P. robustus* and *A. africanus* had diets with similar biomechanical properties, and differences in craniomandibular morphology and enamel thickness are present to compensate for differences in molar morphology.

Finally, it is possible *P. robustus* and *A. africanus* had diets with similar biomechanical properties, and morphological differences are present to compensate for differences in molar biomechanical performance. Despite large levels of overlap, there are differences in dental microwear between *P. robustus* and *A. africanus*. It is possible these differences are not due to consuming different foods, but due to seasonal, environmental and/or population-level variation in the foods consumed (e.g. [23,104,105]). If true, this would imply that there are no significant differences in the biomechanical properties of the foods consumed by these two hominin species.

Our results show that, should *P. robustus* and *A. africanus* have consumed the same foods, *P. robustus* would have required more force and/or energy to breakdown these foods. This would require *P. robustus* to have increased force/energy production (e.g. orthognathism, larger chewing muscles) and thicker enamel (to resist these forces). If hypothesis 3 is true, it highlights the need to use a holistic approach to biomechanical data to reconstruct the ecologies of extinct species.

5. Conclusion

We investigated differences in dental biomechanical function between *P. robustus* and *A. africanus*. Contrary to our expectations, we found *P. robustus* had molars that were less efficient at processing our proxy foods than *A. africanus*. Metrics of biomechanical performance were often correlated to tooth size and wear, but uncorrelated to dental

topographic metrics. When our results are interpreted in conjunction with species averaged morphological, dental microwear and stable carbon isotope data, we see three possible evolutionary scenarios could have occurred (1) *P. robustus* had a more mechanically challenging diet, but inefficient molars because of relaxed selective pressures, (2) *P. robustus* had a more mechanically challenging diet, but inefficient molars because the selection was acting on other aspect(s) of dental morphology and (3) *P. robustus* and *A. africanus* had diets with similar biomechanical properties, and differences in masticatory morphology are present in *P. robustus* to compensate for having inefficient molars.

As with any study, ours has limitations, most of which have to do with our species designations and modelling assumptions. Species designations of the South African material are complex. Some authors would suggest more than one taxa is represented within our *A. africanus* sample (e.g. [68], including *A. prometheus*, or assigning SK 843 to *Homo* as has been done by some researchers, although the assignment of the latter to *Homo* is debated [106]), while others would argue the morphological variation in our sample is due to taxonomic heterogeneity [107]. Within the *P. robustus* sample, some of this heterogeneity may be due to microevolution and that we are time averaging within our sample [108]. The latter interpretation does not strictly assume more than one species is represented by the *P. robustus* or *A. africanus* material. We employ this latter, rather conservative approach in this study, while being fully aware of the caveats. This notwithstanding, several of our modelling assumptions are worth noting. These include using isolated molars instead of tooth rows, a proxy food item unrelated to the foods possibly consumed by these hominins, 3D printing molars in plastic, and therefore not having a sharp enamel ridge, and simplification of masticatory kinematics to a vertical motion. Given the general limitations of the fossil record, and problems associated with producing models of extinct animals, we must be careful with the evolutionary conclusions that can be drawn.

These caveats notwithstanding, the above conclusions cannot be reached by investigating morphological differences in isolation and can only be seen by taking a more holistic approach including experimental testing.

Data accessibility. Raw experimental values are provided in electronic supplementary material, table S3.

The data are provided in the electronic supplementary material [109].

Authors' contributions. M.A.B.:Experimental design, carried out experiments, performed statistical analyses, outlined, wrote and edited manuscript. K.K.: experimental design, outlined, wrote and edited manuscript.

Competing interests. We declare we have no competing interests.

Funding. We received no funding for this study.

Acknowledgements. The authors thank the Max Planck Society for funding this work and prior projects which were conducted within the former Max Planck Weizmann Center for Integrative Archaeology and Anthropology and the Department of Human Evolution, both parts of the Max Planck Institute for Evolutionary Anthropology. For access to the comparative sample and scans of the specimens, we thank Stephany Potze (Ditsong National Museum of Natural History), Bernard Zipfel and Sifelani Jura (University of Witwatersrand) and Jean-Jacques Hublin (Max Planck Institute for Evolutionary Anthropology), as well as Colin Menter and Frances Thackeray. For assistance with scanning of this sample, we thank Kudakwashe Jakata, Matthew Skinner, Frances Thackeray, Heiko Temming, Patrick Schoenfeld, Collin Moore, Tracy Kivell and Adam Sylvester. We thank Franck Guy for providing measurements of the FLS II tester. M.A.B. further thanks the American Association of Physical Anthropology for hosting and funding the symposium on anthroengineering where this research was first presented. He further thanks Patricia Kramer for helping him organize the symposium and this volume. Finally, the authors thank Tim Holt and the Royal Society for agreeing to take on these articles and producing the first special issue on anthroengineering.

Endnote

[1]The measurements for force and energy include the force and energy due to friction between the tooth and the gelatine block. Due to the complex nature of the fracture, it was not possible to subtract out the frictional force [2].

References

1. Ungar PS, Brown CA, Bergstrom TS, Walker A. 2003 Quantification of dental microwear by tandem scanning confocal microscopy and scale-sensitive fractal analyses. *Scanning* **25**, 185–193. (doi:10.1002/sca.4950250405)
2. Lucas PW. 2004 *Dental functional morphology: how teeth work*. Cambridge, UK: Cambridge University Press.
3. Berthaume MA. 2016 Food mechanical properties and dietary ecology. *Am. J. Phys. Anthropol.* **159**, 79–104. (doi:10.1002/ajpa.22903)
4. King SJ, Arrigo-Nelson SJ, Pochron ST, Semprebon GM, Godfrey LR, Wright PC, Jernvall J. 2005 Dental senescence in a long-lived primate links infant survival to rainfall. *Proc. Natl Acad. Sci. USA* **102**, 16 579–16 583. (doi:10.1073/pnas.0508377102)
5. Lucas P, Constantino P, Wood B, Lawn B. 2008 Dental enamel as a dietary indicator in mammals. *Bioessays* **30**, 374–385. (doi:10.1002/bies.20729)
6. Winchester JM, Boyer DM, St Clair EM, Gosselin-Ildari AD, Cooke SB, Ledogar JA. 2014 Dental topography of platyrrhines and prosimians: convergence and contrasts. *Am. J. Phys. Anthropol.* **153**, 29–44. (doi:10.1002/ajpa.22398)
7. Ungar PS. 2010 *Mammal teeth: origin, evolution, and diversity*. JHU Press. See https://books.google.com/books?hl=en&lr=&id=BGGTYS2AgncC&pgis=1.
8. Berthaume MA, Lazzari V, Guy F. 2020 The landscape of tooth shape: over 20 years of dental topography in primates. *Evol. Anthropol.* **29**, 245–262. (doi:10.1002/evan.21856)
9. Berthaume M, Grosse IR, Patel ND, Strait DS, Wood S, Richmond BG. 2010 The effect of early hominin occlusal morphology on the fracturing of hard food items. *Anat. Rec.* **293**, 594–606. (doi:10.1002/ar.21130)
10. Abler W. 1992 The serrated teeth of tyrannosaurid dinosaurs, and biting structures in other animals. *Paleobiology* **18**, 161–183. (doi:10.1017/S0094837300013956)
11. Paine O, Sponheimer M, Henry A, Hutschenreuther A, Leichliter J, Cordon J, Codron D, Loudon J. 2014 Exploring C4 plant foods and their potential as hominin dietary resources: the mechanical properties of savanna vegetation from the Cradle of Humankind, South Africa. *Am. J. Phys. Anthropol.* **153**, 140.
12. Paine OCC, Koppa A, Henry AG, Leichliter JN, Codron D, Codron J, Lambert JE, Sponheimer M. 2018 Grass leaves as potential hominin dietary resources. *J. Hum. Evol.* **117**, 44–52. (doi:10.1016/J.JHEVOL.2017.10.013)
13. Sponheimer M *et al*. 2013 Isotopic evidence of early hominin diets. *Proc. Natl Acad. Sci. USA* **110**, 10 513–10 518. (doi:10.1073/pnas.1222579110)
14. Grine FE, Sponheimer M, Ungar PS, Lee-Thorp J, Teaford MF. 2012 Dental microwear and stable isotopes inform the paleoecology of extinct hominins. *Am. J. Phys. Anthropol.* **148**, 285–317. (doi:10.1002/ajpa.22086)
15. Sponheimer M, Passey BH, de Ruiter DJ, Guatelli-Steinberg D, Cerling TE, Lee-Thorp JA. 2006 Isotopic evidence for dietary variability in the early hominin

Paranthropus robustus. *Science* **314**, 980–982. (doi:10.1126/science.1133827)

16. Sponheimer M, Lee-Thorp JA. 1999 Isotopic evidence for the diet of an early hominid, *Australopithecus africanus*. *Science* **283**, 368–370. (doi:10.1126/science.283.5400.368)
17. Sponheimer M, Lee-Thorp J, de Ruiter D, Codron D, Codron J, Baugh AT, Thackeray F. 2005 Hominins, sedges, and termites: new carbon isotope data from the Sterkfontein valley and Kruger National Park. *J. Hum. Evol.* **48**, 301–312. (doi:10.1016/j.jhevol.2004.11.008)
18. Daegling DJ, Hua L-CC, Ungar PS. 2016 The role of food stiffness in dental microwear feature formation. *Arch. Oral Biol.* **71**, 16–23. (doi:10.1016/j.archoralbio.2016.06.018)
19. Lucas PW *et al.* 2013 Mechanisms and causes of wear in tooth enamel: implications for hominin diets. *J. R. Soc. Interface* **10**, 20120923. (doi:10.1098/rsif.2012.0923)
20. Xia J, Zheng J, Huang D, Tian ZR, Chen L, Zhou Z, Ungar PS, Qian L. 2015 New model to explain tooth wear with implications for microwear formation and diet reconstruction. *Proc. Natl Acad. Sci. USA* **112**, 10 669–10 672. (doi:10.1073/pnas.1509491112)
21. Hua L-C, Brandt ET, Meullenet J-F, Zhou Z-R, Ungar PS. 2015 Technical note: an in vitro study of dental microwear formation using the BITE Master II chewing machine. *Am. J. Phys. Anthropol.* **158**, 769–775. (doi:10.1002/ajpa.22823)
22. Winkler DE, Schulz-Kornas E, Kaiser TM, De Cuyper A, Clauss M, Tütken T. In press. Forage silica and water content control dental surface texture in guinea pigs and provide implications for dietary reconstruction. (doi:10.1073/pnas.1814081116)
23. Schulz-Kornas E, Stuhlträger J, Clauss M, Wittig RM, Kupczik K. 2019 Dust affects chewing efficiency and tooth wear in forest dwelling Western chimpanzees (*Pan troglodytes verus*). *Am. J. Phys. Anthropol.* **169**, 66–77. (doi:10.1002/ajpa.23808)
24. Smith AL *et al.* 2015 The feeding biomechanics and dietary ecology of *Paranthropus boisei*. *Anat. Rec.* **298**, 145–167. (doi:10.1002/ar.23073)
25. Daegling DJ, Judex S, Ozcivici E, Ravosa MJ, Taylor AB, Grine FE, Teaford MF, Ungar PS. 2013 Viewpoints: feeding mechanics, diet, and dietary adaptations in early hominins. *Am. J. Phys. Anthropol.* **151**, 356–371. (doi:10.1002/ajpa.22281)
26. Strait DS *et al.* 2013 Viewpoints: diet and dietary adaptations in early hominins: the hard food perspective. *Am. J. Phys. Anthropol.* **151**, 339–355. (doi:10.1002/ajpa.22285)
27. Scott RS, Ungar PS, Bergstrom TS, Brown CA, Grine FE, Teaford MF, Walker A. 2005 Dental microwear texture analysis shows within-species diet variability in fossil hominins. *Nature* **436**, 693–695. (doi:10.1038/nature03822)
28. Grine FE. 1986 Dental evidence for dietary differences in *Australopithecus* and *Paranthropus*: a quantitative analysis of permanent molar microwear. *J. Hum. Evol.* **15**, 783–822. (doi:10.1016/S0047-2484(86)80010-0)
29. Williams F. 2015 Dietary proclivities of *Paranthropus robustus* from Swartkrans, South Africa. *Anthropol. Rev.* **78**, 1–19. (doi:10.1515/anre-2015-0001)
30. Grine FE *et al.* 2010 Craniofacial biomechanics and functional and dietary inferences in hominin paleontology. *J. Hum. Evol.* **58**, 293–308. (doi:10.1016/j.jhevol.2009.12.001)
31. Constantino PJ, Lee JJ-W, Chai H, Zipfel B, Ziscovici C, Lawn BR, Lucas PW. 2010 Tooth chipping can reveal the diet and bite forces of fossil hominins. *Biol. Lett.* **6**, 826–829. (doi:10.1098/rsbl.2010.0304)
32. Demes B, Creel N. 1988 Bite force, diet, and cranial morphology of fossil hominids. *J. Hum. Evol.* **17**, 657–670. (doi:10.1016/0047-2484(88)90023-1)
33. Rak Y. 1983 *The australopithecine face*, 1st edn. New York, NY: Academic Press. See https://books.google.com/books?hl=en&lr=&id=zS20BQAAQBAJ&pgis=1.
34. Robinson JTT. 1954 Prehominid dentition and hominid evolution. *Evolution* **8**, 324–334. (doi:10.2307/2405779)
35. Skinner MM, Alemseged Z, Gaunitz C, Hublin J-J. 2015 Enamel thickness trends in Plio-Pleistocene hominin mandibular molars. *J. Hum. Evol.* **85**, 35–45. (doi:10.1016/j.jhevol.2015.03.012)
36. Daegling DJ, Grine FE. 1991 Compact bone distribution and biomechanics of early hominid mandibles. *Am. J. Phys. Anthropol.* **86**, 321–339. (doi:10.1002/ajpa.1330860302)
37. Brain C. 1981 *The hunters or the hunted? An introduction to African cave taphonomy*. University of Chicago Press.
38. Kupczik K, Toro-Ibacache V, Macho GA. 2018 On the relationship between maxillary molar root shape and jaw kinematics in *Australopithecus africanus* and *Paranthropus robustus*. *R. Soc. Open Sci.* **5**, 180825. (doi:10.1098/RSOS.180825)
39. Ungar PS. 2007 Dental topography and human evolution with comments on the diets of *Australopithecus africanus* and *Paranthropus*. In *Dental perspectives on human evolution* (eds SE Bailey, J-J Hublin), pp. 321–343. Dordrecht, The Netherlands: Springer.
40. Berthaume MA, Delezene LK, Kupczik K. 2018 Dental topography and the diet of *Homo naledi*. *J. Hum. Evol.* **118**, 14–26. (doi:10.1016/j.jhevol.2018.02.006)
41. Marshall AJ, Wrangham RW. 2007 Evolutionary consequences of fallback foods. *Int. J. Primatol.* **28**, 1219–1235. (doi:10.1007/s10764-007-9218-5)
42. Jolly CJ. 1970 The seed-eaters: a new model of hominid differentiation based on a baboon analogy. *Man* **5**, 5–26. (doi:10.2307/2798801
43. Walker A. 1981 Diet and teeth: dietary hypotheses and human evolution. *Phil. Trans. R. Soc. B* **292**, 57–64. (doi:10.1098/rstb.1981.0013)
44. Dominy NJ, Vogel ER, Yeakel JD, Constantino P, Lucas PW. 2008 Mechanical properties of plant underground storage organs and implications for dietary models of early hominins. *Evol. Biol.* **35**, 159–175. (doi:10.1007/s11692-008-9026-7)
45. Wood B, Strait D. 2004 Patterns of resource use in early Homo and Paranthropus. *J. Hum. Evol.* **46**, 119–162. (doi:10.1016/j.jhevol.2003.11.004)
46. Joannes-Boyau R *et al.* 2019 Elemental signatures of *Australopithecus africanus* teeth reveal seasonal dietary stress. *Nature* **572**, 112–115.
47. McKee JK. 1989 Australopithecine anterior pillars: reassessment of the functional morphology and phylogenetic relevance. *Am. J. Phys. Anthropol.* **80**, 1–9. (doi:10.1002/ajpa.1330800102)
48. Strait DS *et al.* 2009 The feeding biomechanics and dietary ecology of *Australopithecus africanus*. *Proc. Natl Acad. Sci. USA* **106**, 2124–2129. (doi:10.1073/pnas.0808730106)
49. Spears IR, Crompton RH. 1994 Finite elements stress analysis as a possible tool for reconstruction of hominid dietary mechanics. *Z. Morphol. Anthropol.* **80**, 3–17. (https://www.jstor.org/stable/25757414)
50. Evans AR, Sanson GD. 1998 The effect of tooth shape on the breakdown of insects. *J. Zool.* **246**, 391–400. (doi:10.1111/j.1469-7998.1998.tb00171.x)
51. Ang KY, Lucas PW, Tan HTW. 2006 Incisal orientation and biting efficiency. *J. Hum. Evol.* **50**, 663–672. (doi:10.1016/j.jhevol.2006.01.003)
52. Anderson PSL, Rayfield EJ. 2012 Virtual experiments, physical validation: dental morphology at the intersection of experiment and theory. *J. R. Soc. Interface* **9**, 1846–1855. (doi:10.1098/rsif.2012.0043)
53. Anderson PSL, LaBarbera M. 2008 Functional consequences of tooth design: effects of blade shape on energetics of cutting. *J. Exp. Biol.* **211**, 3619–3626. (doi:10.1242/jeb.020586)
54. Freeman PW, Lemen CA. 2006 Puncturing ability of idealized canine teeth: edged and non-edged. **269**, 51–56. (doi:10.1111/j.1469-7998.2006.00049.x)
55. Berthaume MA, Dumont ER, Godfrey LR, Grosse IR. 2013 How does tooth cusp radius of curvature affect brittle food item processing? *J. R. Soc. Interface* **10**, 20130240. (doi:10.1098/rsif.2013.0240)
56. Berthaume MA, Dumont ER, Godfrey LR, Grosse IR. 2014 The effects of relative food item size on optimal tooth cusps sharpness during brittle food item processing. *J. R. Soc. Interface* **11**, 20140965. (doi:10.1098/rsif.2014.0965)
57. Ledogar JA, Winchester JM, St Clair EM, Boyer DM. 2013 Diet and dental topography in pitheciine seed predators. *Am. J. Phys. Anthropol.* **150**, 107–121. (doi:10.1002/ajpa.22181)
58. Ungar PS, M'Kirera F. 2003 A solution to the worn tooth conundrum in primate functional anatomy. *Proc. Natl Acad. Sci. USA* **100**, 3874–3877. (doi:10.1073/pnas.0637016100)
59. Bunn JM, Boyer DM, Lipman Y, St Clair EM, Jernvall J, Daubechies I. 2011 Comparing Dirichlet normal surface energy of tooth crowns, a new technique of molar shape quantification for dietary inference, with previous methods in isolation and in combination. *Am. J. Phys. Anthropol.* **145**, 247–261. (doi:10.1002/ajpa.21489)
60. Patel ND, Grosse I, Sweeney D, Strait DS, Lucas PW, Wright B, Godfrey LR. 2008 An efficient method for predicting fracture of hard food source. In *Volume 2: biomedical and biotechnology engineering*, pp. 521–528. ASME.
61. Skamniotis CG, Kamaludin MA, Elliott M, Charalambides MN. 2017 A novel essential work of fracture experimental methodology for highly dissipative materials. *Polymer* **117**, 167–182. (doi:10.1016/j.polymer.2017.03.057)

62. Skamniotis CG, Elliott M, Charalambides MN. 2019 Computer simulations of food oral processing to engineer teeth cleaning. *Nat. Commun.* **10**, 3571. (doi:10.1038/s41467-019-11288-5)
63. Kay RF. 1975 The functional adaptations of primate molar teeth. *Am. J. Phys. Anthropol.* **43**, 195–216. (doi:10.1002/ajpa.1330430207)
64. Sheine WS, Kay RF. 1977 An analysis of chewed food particle size and its relationship to molar structure in the primates *Cheirogaleus medius* and *Galago senegalensis* and the insectivoran *Tupaia glis*. *Am. J. Phys. Anthropol.* **47**, 15–20. (doi:10.1002/ajpa.1330470106)
65. Boyer DM. 2008 Relief index of second mandibular molars is a correlate of diet among prosimian primates and other euarchontan mammals. *J. Hum. Evol.* **55**, 1118–1137. (doi:10.1016/j.jhevol.2008.08.002)
66. Godfrey LR, Winchester JM, King SJ, Boyer DM, Jernvall J. 2012 Dental topography indicates ecological contraction of lemur communities. *Am. J. Phys. Anthropol.* **148**, 215–227. (doi:10.1002/ajpa.21615)
67. Allen KL, Cooke SB, Gonzales LA, Kay RF. 2015 Dietary inference from upper and lower molar morphology in platyrrhine primates. *PLoS ONE* **10**, e0118732. (doi:10.1371/journal.pone.0118732)
68. Clarke RJ, Kuman K. 2019 The skull of StW 573, a 3.67 Ma *Australopithecus prometheus* skeleton from Sterkfontein Caves, South Africa. *J. Hum. Evol.* **134**, 102634. (doi:10.1016/j.jhevol.2019.06.005)
69. Scott EC. 1979 Dental wear scoring technique. *Am. J. Phys. Anthropol.* **51**, 213–217. (doi:10.1002/ajpa.1330510208)
70. Pampush JD, Spradley JP, Morse PE, Griffith D, Gladman JT, Gonzales LA, Kay RF. 2018 Adaptive wear-based changes in dental topography associated with atelid (Mammalia: Primates) diets. *Biol. J. Linn. Soc.* **124**, 584–606. (doi:10.1093/biolinnean/bly069)
71. EDF R&D TP. 2013 CloudCompare [GPL Software] (version2.6.0). See http://www.cloudcompare.org/
72. Stratasys. In press. Rigid Translucent (RGD720). See https://www.javelin-tech.com/3d/stratasys-materials/rigid-translucent/
73. Johnson KL, Johnson KL. 1987 *Contact mechanics*. Cambridge University Press. See https://books.google.com/books?hl=en&lr=&id=oy-P5D7hTVAC&pgis=1.
74. Sui Z, Agrawal KR, Corke H, Lucas PW. 2006 Biting efficiency in relation to incisal angulation. *Arch. Oral Biol.* **51**, 491–497. (doi:10.1016/j.archoralbio.2005.11.002)
75. Conith AJ, Imburgia MJ, Crosby AJ, Dumont ER. 2016 The functional significance of morphological changes in the dentitions of early mammals. *J. R. Soc. Interface* **13**, 20160713.
76. Freeman P, Weins W. 1997 Puncturing ability of bat canine teeth: the tip. *Mammal. Pap. Univ. Nebraska State Museum.*
77. Mai Y-W, Atkins AG. 1989 Further comments on J-shaped stress-strain curves and the crack resistance of biological materials. *J. Phys. D Appl. Phys.* **22**, 48–54. (doi:10.1088/0022-3727/22/1/007)
78. Kendall K, Fuller KNG. 1987 J-shaped stress/strain curves and crack resistance of biological materials. *J. Phys. D Appl. Phys.* **20**, 1596–1600. (doi:10.1088/0022-3727/20/12/008)
79. M'Kirera F, Ungar PS. 2003 Occlusal relief changes with molar wear in *Pan troglodytes troglodytes* and *Gorilla gorilla gorilla*. *Am. J. Primatol.* **60**, 31–41. (doi:10.1002/ajp.10077)
80. Evans AR, Wilson GP, Fortelius M, Jernvall J. 2007 High-level similarity of dentitions in carnivorans and rodents. *Nature* **445**, 78–81. (doi:10.1038/nature05433)
81. Berthaume MA, Winchester J, Kupczik K. 2019 Ambient occlusion and PCV (portion de ciel visible): a new dental topographic metric and proxy of morphological wear resistance. *PLoS ONE* **14**, e0215436. (doi:10.1371/journal.pone.0215436)
82. Winchester JM. 2016 MorphoTester: an open source application for morphological topographic analysis. *PLoS ONE* **11**, e0147649. (doi:10.1371/journal.pone.0147649)
83. Berthaume MA, Winchester J, Kupczik K. 2019 Effects of cropping, smoothing, triangle count, and mesh resolution on 6 dental topographic metrics. *PLoS ONE* **14**, e0216229. (doi:10.1371/JOURNAL.PONE.0216229)
84. Berthaume MA, Schroer K. 2017 Extant ape dental topography and its implications for reconstructing the emergence of early Homo. *J. Hum. Evol.* **112**, 15–29. (doi:10.1016/j.jhevol.2017.09.001)
85. Taylor GK, Thomas ALR. 2014 *Evolutionary biomechanics*. Oxford, UK: Oxford University Press.
86. Swan K. 2016 *Dental morphology and mechanical efficiency during development in a hard object feeding primate* (*Cercocebus atys*). University of York.
87. Berthaume MA. 2016 On the relationship between tooth shape and masticatory efficiency: a finite element study. *Anat. Rec.* **299**, 679–687. (doi:10.1002/ar.23328)
88. McElreath R. 2016 rethinking: Statistical Rethinking book package. R package version 1.59.
89. RStudio Team. 2016 RStudio: Integrated Development Environment for R.
90. Prufrock KA, Boyer DM, Silcox MT. 2016 The first major primate extinction: an evaluation of paleoecological dynamics of North American stem primates using a homology free measure of tooth shape. *Am. J. Phys. Anthropol.* **159**, 683–697. (doi:10.1002/ajpa.22927)
91. Evans AR. 2013 Shape descriptors as ecometrics in dental ecology. *Hystrix Ital. J. Mammal.* **24**, 133–140. (doi:10.4404/hystrix-24.1-6363)
92. Guy F, Lazzari V, Gilissen E, Thiery G. 2015 To what extent is primate second molar enamel occlusal morphology shaped by the enamel-dentine junction? *PLoS ONE* **10**, e0138802. (doi:10.1371/journal.pone.0138802)
93. Thiery G, Guy F, Lazzari V. 2017 Investigating the dental toolkit of primates based on food mechanical properties: feeding action does matter. *Am. J. Primatol.* **79**, 22640. (doi:10.1002/ajp.22640)
94. Sheine WS, Kay RR. 1982 A model for comparison of masticatory effectiveness in primates. *J. Morphol.* **172**, 139–149. (doi:10.1002/jmor.1051720202)
95. Kay RF, Sheine WS. 1979 On the relationship between chitin particle size and digestibility in the primate *Galago senegalensis*. *Am. J. Phys. Anthropol.* **50**, 301–308. (doi:10.1002/ajpa.1330500303)
96. Teaford MF, Ungar PS. 2000 Diet and the evolution of the earliest human ancestors. *Proc. Natl Acad. Sci. USA* **97**, 13 506–13 511. (doi:10.1073/pnas.260368897)
97. Ross CF, Iriarte-Diaz J. 2014 What does feeding system morphology tell us about feeding? *Evol. Anthropol.* **23**, 105–120. (doi:10.1002/evan.21410)
98. Constantino PJ *et al.* 2011 Adaptation to hard-object feeding in sea otters and hominins. *J. Hum. Evol.* **61**, 89–96.
99. Pampush JD, Duque AC, Burrows BR, Daegling DJ, Kenney WF, McGraw WS. 2013 Homoplasy and thick enamel in primates. *J. Hum. Evol.* **64**, 216–224.
100. Vogel ER, van Woerden JT, Lucas PW, Utami Atmoko SS, van Schaik CP, Dominy NJ. 2008 Functional ecology and evolution of hominoid molar enamel thickness: pan troglodytes schweinfurthii and *Pongo pygmaeus wurmbii*. *J. Hum. Evol.* **55**, 60–74. (doi:10.1016/j.jhevol.2007.12.005)
101. Smith TM *et al.* 2013 Dental ontogeny in Pliocene and early Pleistocene hominins. *PLoS ONE* **10**, e0118118. (doi:10.1371/journal.pone.0118118)
102. Guy F, Gouvard F, Boistel R, Euriat A, Lazzari V. 2013 Prospective in (Primate) dental analysis through tooth 3D topographical quantification. *PLoS ONE* **8**, e66142. (doi:10.1371/journal.pone.0066142)
103. Skinner MM *et al.* 2010 Brief communication: contributions of enamel-dentine junction shape and enamel deposition to primate molar crown complexity. *Am. J. Phys. Anthropol.* **142**, 157–163.
104. Stuhlträger J, Schulz-Kornas E, Wittig RM, Kupczik K. 2019 Ontogenetic dietary shifts and microscopic tooth wear in Western Chimpanzees. *Front. Ecol. Evol.* **7**, 298. (doi:10.3389/fevo.2019.00298)
105. Carlson BA, Kingston JD. 2014 Chimpanzee isotopic ecology: a closed canopy C3 template for hominin dietary reconstruction. *J. Hum. Evol.* **76**, 107–115.
106. Grine FE. 2005 Early Homo at Swartkrans, South Africa: a review of the evidence and an evaluation of recently proposed morphs. *S. Afr. J. Sci.* **101**, 43–52.
107. Grine FE. 2013 The Alpha Taxonomy of *Australopithecus africanus*. In *The paleobiology of australopithecus, paleobiology and paleoanthropology* (eds K Reed, JG Fleagle, RE Leakey), pp. 73–104. Dordrecht, the Netherlands: Springer Science and Business Media.
108. Martin JM *et al.* 2020 Drimolen cranium DNH 155 documents microevolution in an early hominin species. *Nat. Ecol. Evol.* **5**, 38–45 (doi:10.1038/s41559-020-01319-6)
109. Berthaume MA, Kupczik K. 2021 Molar biomechanical function in South African hominins *Australopithecus africanus* and *Paranthropus robustus*. Figshare.